RESEARCH ON THE DYNAMIC STATE OF RIVER-MOUTH BAR UNDER FLOOD CONDITIONS IN THE YURAGAWA RIVER

TAKAHARU OCHI[(1)], KEIICHI KANDA[(2)] , HIROSHI MIWA[(3)] & FUMINORI NAKAMURA[(4)]

[(1)] *Graduate Student, Department of Civil Engineering, National Institute of Technology, Akashi, Japan, ac1406@s.akashi.ac.jp*

[(2)] *Professor, Department of Civil Engineering, National Institute of Technology, Akashi, Japan, kanda@akashi.ac.jp*

[(3)] *Professor, Department of Civil Engineering and Architecture , National Institute of Technology, Maizuru, Japan, miwa@maizuru-ct.ac.jp*

[(4)] *Assistant Professor, Department of Civil Engineering, National Institute of Technology, Akashi, Japan, nakamura@akashi.ac.jp*

ABSTRACT

The topography of a sand bar is continuously affected by river runoff, ocean currents and sea wave action. Disruptions in any of these factors can alter the geometry of the sand bar, causing sedimentation problems and increased risk of flooding. In order to mitigate the risks associated with such changes, it is important to understand the characteristics of the topographic changes of river-mouth bars, and to develop a method for controlling the bar geometry. This study examined the effect of variations in the geometric properties of a river-mouth bar using hydrological data (river water discharge and sea wave height). The application of spur dikes to promote erosion of the sand bar by altering the direction of river flow was evaluated by means of flume experiments. A two-dimensional numerical model (iRIC Project) was also applied to examine the effectiveness of spur dikes on river-mouth bar control. The results of this study clarified the efficiency of measures for managing sand bar formation at the mouth of the Yuragawa River in Kyoto Prefecture, Japan.

Keywords: , river-mouth bar, topographical changes, spur dike, flume experiment, numerical simulation

1. INTRODUCTION

The topology of river mouths, which are defined as regions where river runoff enters an ocean, is characterized by the combined influence of sediment transported by the river and near shore currents associated with tides and sea waves. River mouths along the coast of the Sea of Japan are particularly affected by the action of winter sea waves, and tidal prisms are small. Under these conditions, river-mouth bars tend to develop under conditions of longshore sediment transport, and blocking of river-mouths is frequent. Floods tend to breach the river-mouth bars that develop during dry periods, and complex changes occur in bar behavior during floods and in post-flushing river-mouth channel width. These changes vary depending on flood hydrodynamics, fluvial morphology near the river mouth, and the presence or absence of harbor facilities and other man-made structures along the coast.

Hosoyamada et al. (2006) examined the changes in river-mouth bar morphology during flash flooding by numerical analysis using nonlinear shallow-wave modeling, and quantitatively assessed the stage-lowering effect of sediment flushing, in their study on the river-mouth bars of the Aganogawa River, which were not effectively breached by flooding on a scale of approximately 50% of its design discharge (i.e. 6,000 m^3/s). Kuwahara et al. (1996) also performed a two-dimensional analysis of riverbed changes in the Natori River. In response to the strong three-dimensional flow field in the periphery of a river-mouth bar with a complex geometry, Tateyama et al. (1995) recently developed a new analytical method (referred to as the bottom velocity computation (BVC) method) to assess bottom flow velocities without any assumptions of shallow flow, and applied the BVC to analyze and reproduce the changes in bar morphology that occurred during the flooding that occurred in the Aganogawa River flood in 2011 (flow discharge approximately 11,000 m^3/s).

On the other hand, in their study on river-mouth channel width of rivers with river-mouth bars, Sato et al. (2004) modeled sediment transport by near shore currents associated with sea waves and tides, as well as by river runoff, and derived predictions of the channel width for different equilibrium states. However, as shown in the results of this study, bar dynamics in times of flooding are affected by the pre-flood fluvial morphology, coastal sea level, and flood discharge. In many cases, the bar is not completely flushed out, even in design-scale floods.

In the Yuragawa River located Kyoto Prefecture in Japan, the topographical change at the river-mouth consists of complicated interactions of river and marine forces. In October 2004, a large part of the river-mouth bar was eroded by the flood flow of typhoon No.23. Since then, the river-mouth bar has developed on the right bank only, and the river-mouth channel has been fixed along the left bank. This situation may cause some problems such as bank erosion, washout of bank protection works and harmful effects on other coastal structures. Effects of water discharge during flood periods on the river-mouth bar responses are also not clarified. Therefore, the risk of a high water levels caused by the river-mouth clogging is formidable. In order to avoid these problems and risk, it is important to understand the

characteristics of the topographical changes of the river-mouth bar and their causes, and to propose a control method of the bar geometry.

In this study, the temporal variations in geometrical properties (e.g., bar area and shape) of the river-mouth bar were analyzed on the basis of the hydrological and topographical data in the Yuragawa River estuary. The effects of the river water discharge and the sea wave height on the geometrical properties of the bar were investigated. As for the bar control, the effectiveness of a spur dike, which could change the flow direction of erosion from the bar, was evaluated by means of flume experiments. The two-dimensional numerical model was also applied to further investigate the effects of the spur dike on the bar control. The simulation results were verified against the experimental results.

2. FIELD MEASUMENT ON DYNAMIC STATE OF RIVER MOUTH TOPHOGRAPHY

2.1 Outline of the Yuragawa River

The Yuragawa River is located in the north of Kyoto Prefecture, in the mid-west in Japan, as shown in Figure1. The origin of the river is Mikunidake situated on the borders of three prefectures of Kyoto, Fukui and Shiga. The length of the river is 146 km, and the size of its basin is 1,880 km^2. The Yuragawa river system is one of the 109 Class A river systems in Japan. The Yuragawa River can be classified into three reaches. In the upper reaches, V-shaped ravines and river terraces have developed. The width of river increases in the middle reaches and pools and riffles are developed in the main channel of the river. The lower reaches consist of the valley plain, the stream flows along the long and narrow bottom of the mountains. Figure 2 shows the longitudinal bed profile of the lower and middle reaches of the Yuragawa River. The average bed gradient around Fukuchiyama (37 km away from the river-mouth) in the middle reaches is about 1/1,500, whereas the bed gradient in the lower reaches is approximately 1/6,000 to 1/8,000. Therefore, the length of tidal section of the river reaches over 20 km.

Figure 1. Location and basin of the Yuragawa River

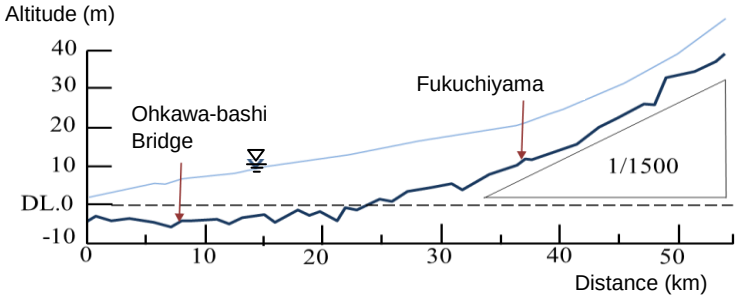

Figure 2. Longitudinal bed profile of lower and middle reaches

2.2 Changes of river-mouth topography for 60 years

Figure 3 shows the changes of river-mouth topography from 1947 to 2009. In 1947 and 1963, the river-mouth bar on the right bank was developed considerably and the width of the river-mouth channel was approximately 80-100 m. The river-mouth bar on the right bank was disappeared and it on the left bank was developed in 1972. The river-mouths on the both bank were developed in 1975 and 1982. The widths of the river-mouth channel were approximately 80 m for both years. After that, a large part of the river-mouth bar was flushed out by the flood flow (peak discharge Q_p=3,600 m^3/s) of the typhoon No.10 in 1982 and 1983, the width of the river mouth channel increased to about 300 m. However, the river-mouth bars were developed as shown in photographs of 1986 to 2001. A large part of the river-mouth bar was flushed out again by the flood flow (peak discharge Q_p=5,400 m^3/s) of the typhoon No.23 in 2004. The river-mouth bar has developed on the right bank only after then, and the river-mouth channel has been fixed along the left bank (2009). The construction works of detached breakwaters have been carried out from 1967 and there are 8 detached breakwaters for each bank. The formation of tombolo is confirmed after 1982. Effects of the detached breakwaters on river-mouth bar formation are not clarified.

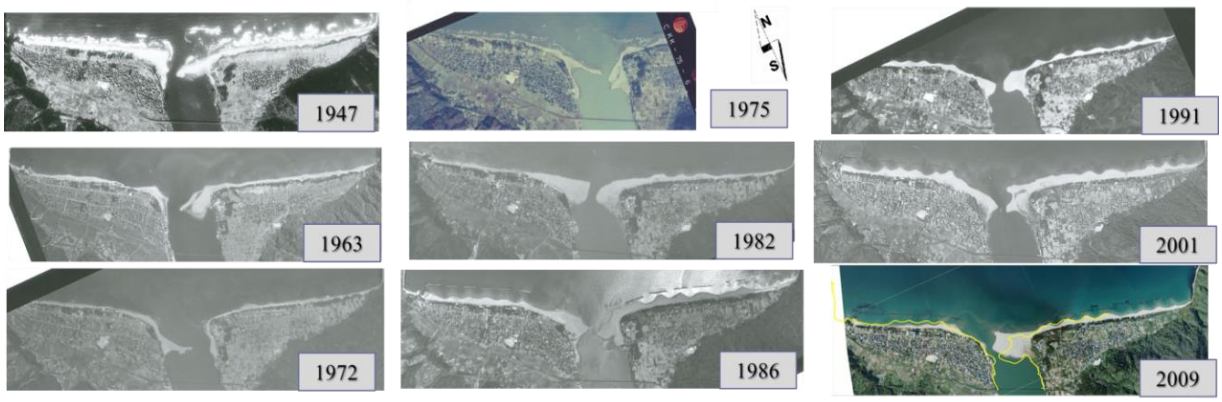

Figure 3.Temporal changes of river-mouth topography in the Yuragawa River (1947-2009)

2.3 Results of fields measurement

In order to clarify the effects of river flow discharge and sea wave height on changes in river-mouth topography, survey works were conducted by using GPS periodically. A surveyor walked along the shore line receiving the satellite signals, and registered the signal to the controller at intervals of approximately 10 to 20 m. The number of stations for each survey was about 70 to 100. The area of the bar and its shape were calculated by means of identifying the coordinates of the stations. Basically, the survey was conducted once a month.

Figure 4 shows (a) the temporal variations in the area of the river-mouth bar, (b) the significant wave height at Kyoga-Misaki (30 km far from the river-mouth) and (c) the water discharge at Fukuchiyama for four years (from May 2010 to April 2014). The datum level was the sea surface at each measurement time, and there was no correction of the datum level because the tidal range was at most 30 cm. The river-mouth bar on the left bank has developed since December 2012 (The survey was started in March 2013). In Figure 4(a), the area of the bar on the right bank shows increases and decreases in the short term, whereas it gradually decreases as a long term tendency. The decreasing rate of the area for four years is approximately 40%. From the short term tendency, it can be seen that the area increased in the winter seasons of 2010, 2012 and 2013, and it decreased in the rainy and summer seasons of 2011 and 2013. As shown in Figure 4(b), Kanda et al. (2012) clarified that the significant wave height over 2.55 m influences the development of the river-mouth bar. Therefore, it can be considered that an increase in the onshore sediment transport may contribute to the increase of the area of the river-mouth bar. A possible reason why the area did not increase in the winter season of 2011 is that the onshore transported sediment from the foreshore may be accumulated on the seabed, where it was eroded by the flood flow in the fall season of 2011. On the other hand, as shown in Figure 4(c), the water discharge over 1,500 m^3/s was recorded a total of four times in the summer seasons of 2011 and 2013. In particular, the flood with discharge of about 5,500 m^3/s occurred due to the typhoon No.18 in September 2013. The area of the bar was reduced by 17% in 2011 and by 40% in 2013 due to these large flood discharges.

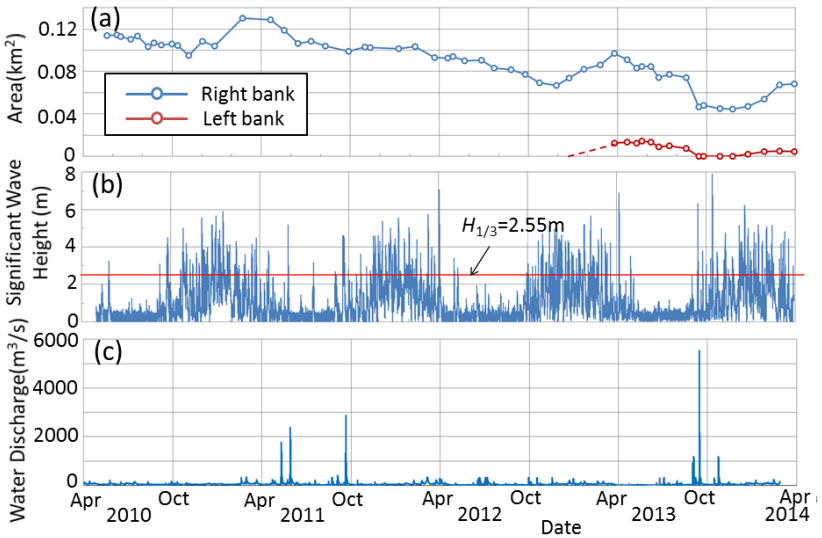

Figure 4. Temporal variations in (a)river-mouth bar area, (b)significant wave height at Kyoga-Misaki and (c)water discharge at Fukuchiyama in the Yuragawa River

3. FLUME EXPERIMENT

3.1 Experimental set-up and procedure

Flume experiments using the large channel, which was modeled based on the Yuragawa River, were conducted in order to clarify the mechanisms of the river bed variation process at the river mouth, and the effects of the spur dikes on the control of the river-mouth bar topography. The experiments were conducted in a horizontal rectangular open channel, which was 8.75 m long and 2.87 m wide as shown in Figure 5. The width of this channel corresponds with the 1/150 scale of the Yuragawa River. The channel has a water level adjusting weir in the returning flume in order to control the water elevation at the downstream end of the channel. Nearly uniform coal dust was used in the experiments as bed sediment. The coal dust had a mean grain diameter d_m of 1.3 mm and a specific gravity σ_s of 1.47.

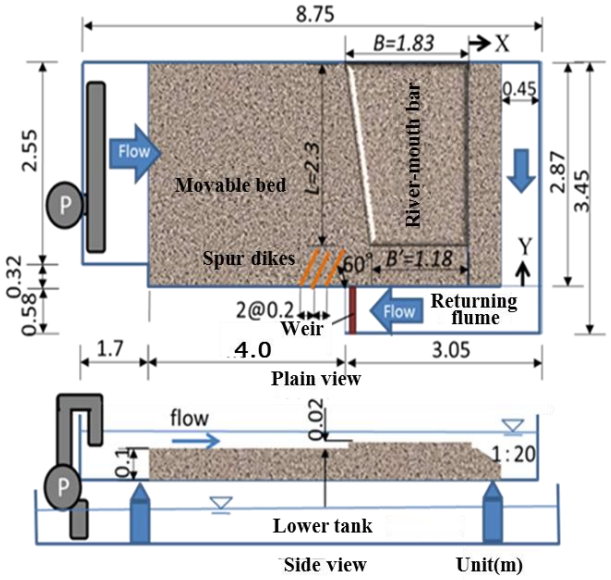

Figure 5. Experimental set-up

The movable bed was flattened with a scraper and the river mouth-bar model, which was modeled based on the results of the topographical survey, was formed on the channel bed. The river mouth-bar is located on the right bank in the Yuragawa River, but the river-mouth model was set to the left bank in order to avoid the effect of the lateral flow toward the returning flume. The height of the river-mouth bar was 0.02 m, the sea bed behind the river-mouth bar was set to a slope I_b of 0.05 (1/20). The other part of the bed was made horizontally.

The experimental conditions are listed in Table 1. In the table, Q = water discharge, Q_c = corresponding water discharge, T = experiment duration, h_d = water surface elevation at the downstream end of the channel, L = length of the spur dike. The discharges in the experiments correspond with the flood discharge of Q = 1,800 to 4,900 m^3/s. The experiment duration (T=20min) corresponds with the peak discharge duration of T = 3.7 hours. In Runs 12B and 12C, the spur dikes were made of plywood, and their thickness and height were 0.01 m and 0.12 m, respectively. Their lengths were either 0.3 m or 0.6 m. Three pieces of spur dike were set on the right bank at intervals of 0.2 cm and placed at an angle of 60 degrees to the wall as shown in Figure 5.

Table 1. Experimental conditions

	Water Discharge Q(l/s)	Corresponding Water Discharge Q_C(m^3/s)	Experiment Duretion T(min)	Water Surface Elevation Downstream End h_d(m)	Length of Spuar Dike L(m)
Run9A	15.0	4,100	20	0.141	None
Run9B	15.0	4,100	20	0.125	None
Run10A	17.8	4,900	20	0.152	None
Run10B	17.8	4,900	20	0.139	None
Run10C	17.8	4,900	20	0.127	None
Run10D	17.8	4,900	20	0.117	None
Run11A	6.7	1,800	20	0.134	None
Run11B	6.5	1,800	20	0.123	None
Run12A	10.8	2,900	20	0.143	None
Run12B	10.7	2,900	20	0.147	0.3
Run12C	10.0	2,900	20	0.139	0.6

In the experiment, the water was stored slowly in the channel in order to avoid erosion of the bed. The prescribed water discharge was fed into the channel after that. The water surface elevation at the downstream end of the channel was controlled by the water level adjusting weir. Water surface elevations were measured with a point gauge, at intervals of 1 m in the longitudinal direction at the location of Y = 0.8 m of the channel before stopping the flow. The motion of PVC particles (particle size = 0.05 mm) on the water surface was recorded by using a video camera for 20 seconds during the experiment. The surface velocity was obtained from PIV analysis (Fujita et al., 1998). Transverse profiles of the bed surface were measured with a laser sensor mounted on a propelled carriage, at intervals of 4 cm in the longitudinal direction of the channel after stopping the flow. The datum plane for water surface and bed surface elevations was set to the channel-bed surface. Then, initial bed elevation was 0.1 m for the river bed part and was 0.12 m for the river-mouth bar part.

The grain size of the river-bed material in the experimental model was larger than that for a scaled-grain replica of the field-site sediment, as its reduction to the scale of 1/150 would have required a grain size of 0.2 mm or less, which would have resulted in suspended-sediment and sand-wave predominance. In this large-grained, and consequently, distorted scale model, similitude (Shields similitude) in the sediment discharge rate was not completely satisfied. In view of the important influence of the critical tractive force of the river-bed material on sediment transport and changes in the river bed around the bar during overflow, we used uniform coal grains with a density of 1.47 g/cm^3 and a mean grain size of d=1.3 mm as the river-bed material, to obtain a correspondence between the river site and the model in the ratio of the shear velocity of the flow to the critical shear velocity of the river-bed material. The critical shear velocity in the model, as calculated by Iwagaki's equation (Iwagaki,1956), was u_{*c}=1.44 cm/s. Experimental measurement of the shear velocity u_* of the flow in the region upstream of the bar yielded values in the range u_*=2.01-2.83 cm/s and thus a u_*/u_{*c} ratio of approximately 1.4-2.0, indicating the occurrence of a dynamic state throughout that range. Application of these values to river-site flood conditions yielded a grain size d of approximately 20 mm, which corresponded closely to the maximum grain size of the river-bed material at the river site (mean grain size of 1.24 mm, maximum grain size of 18 mm).

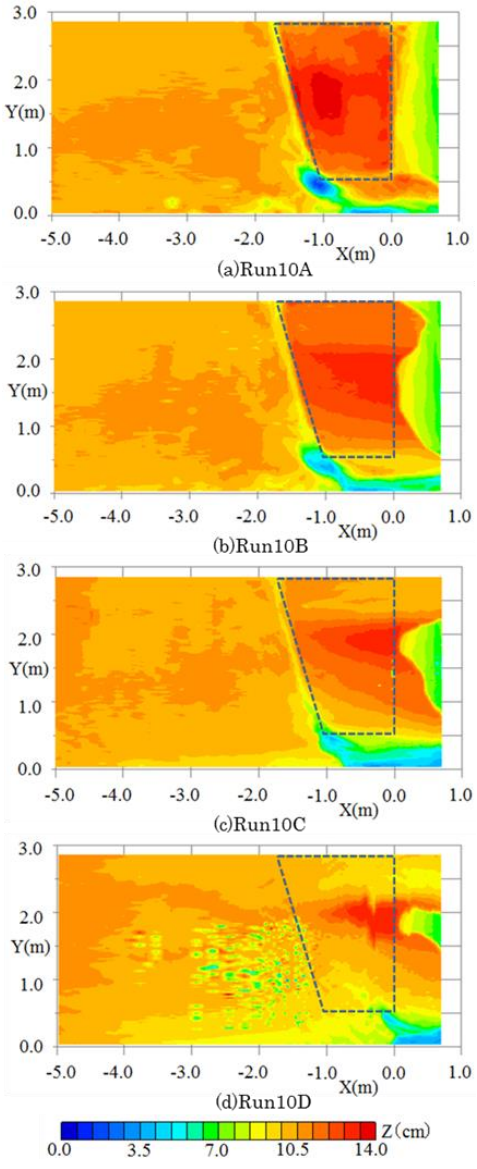

Figure 6. River-bed geometry (Runs 10A – Run10D)

3.2 Experimental results and discussion

Figure 6 shows the river-bed geometry after water passage with a discharge of Q=17.8 l/s and various downstream-end water levels (Runs 10A-10D). This corresponds to a discharge of approximately 4,900 m^3/s at the river-site channel. Figure 7 shows the water level at Y=0.8 m during water passage. As indicated by these figures, in Run 10A, with its high downstream-end water level, the stream completely overflowed the bar but the flow in the overflow region was moderate and no observable river-bed lowering of the bar occurred. The region upstream of the bar was dominated by a meandering flow from near the right bank toward the bar opening. Accompanying the meandering channel formation, the flow converged at the channel and a deeply scoured topography developed upstream of the bar tip. In Run 10B, with its lower downstream-end water level, the flow into the channel was faster and the channel width was wider. In Run 10C, the water-surface gradient increased on the bar and the river bed was lowered, and a depositional landform developed downstream in the sea area. It was found that with the increased water discharge, the rate of bar erosion was greater than that in Run 9B, in which the downstream-end water level was similar. In Run 10D, with its downstream-end water level being lower than the initial bar elevation, the bar was almost entirely eroded and washed away. This is presumably due to the occurrence of a smaller discharge cross section and a higher flow velocity (surface flow velocity ≥30 cm/s in all regions) due to the lower downstream-end water level. For Runs 10A-10C, the area of deep scouring in the channel shifted downstream as the downstream-end water level decreased.

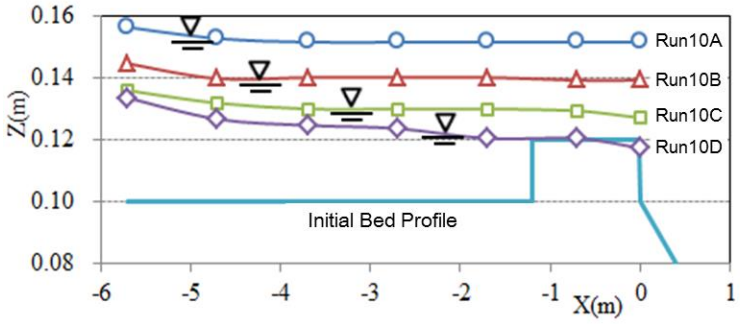

Figure 7. Water level at Y=0.8 m during water passage (Runs 10A – Run10D)

Figure 8 shows the relationship between the downstream-end water level h_d and the channel width B_O for different water discharges. Here, the channel width was taken as the mean value of the transverse distance from the right bank at the river mouth (X=0-1 m), when the bed level was ≤10 cm. As shown in the figure, the channel width tended to increase with decreasing downstream-end water level and increasing water discharge, which is in accordance with the analytical results obtained by Kuwahara(1996) in their investigation of the effect of changes in tidal level during flooding on the phenomenon of river-mouth bar collapse.

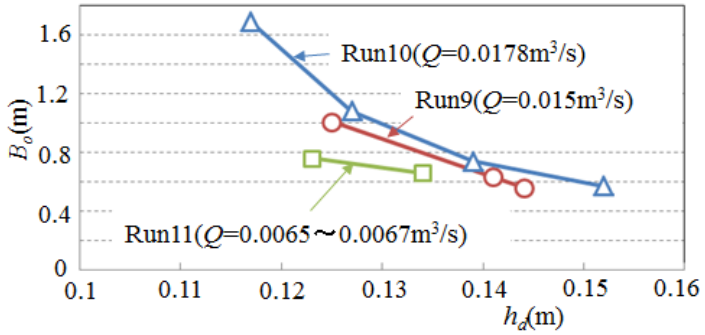

Figure 8. Relationship between the downstream-end water level h_d and the channel width B_0

Figure 9 illustrates the change of river-mouth bar topography by the spur dikes. The area surrounded by the broken line shows the initial shape of the river-mouth bar. The surface velocity distributions around the river-mouth bar are also shown in Figure 10. In the case of no spur dikes (Run 12A), the flow converges toward the river-mouth on the right bank, and progresses erosion of the river-mouth channel. Although the flow gets over the river-mouth bar, the erosion of its surface hardly occurs because its velocity is relatively slow. In the case of the short spur dikes (Run 12B), the converged flow toward the river-mouth is weakened by setting up the spur dikes. And, the front part of the river-mouth bar is eroded more by the redirected flow due to the spur dikes. The erosion of the bar surface hardly occurs in this case too. In the case of the long spur dikes (Run 12C), the scour depth of the river-mouth channel becomes small because the spur dikes strongly redirect the flow toward the river-mouth bar. The redirected flow erodes the river-mouth bar in this case. It is found that the sediments deposit at the lower part of the spur dikes because the flow intensity is weak there. The flow gets over the river-mouth bar and erodes its surface. From the information above, it is considered that the spur dike work is effective for the control of the river-mouth bar

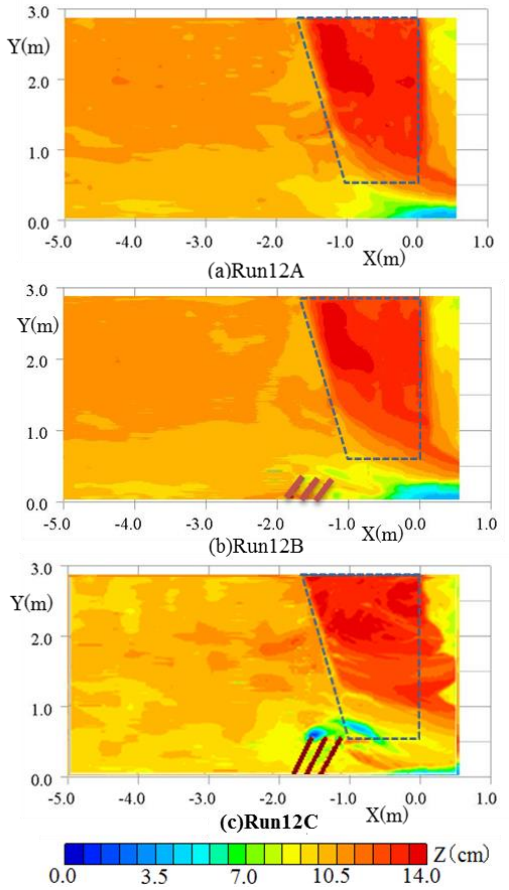

Figure 9. Changes of river-mouth bar topography by spur dikes

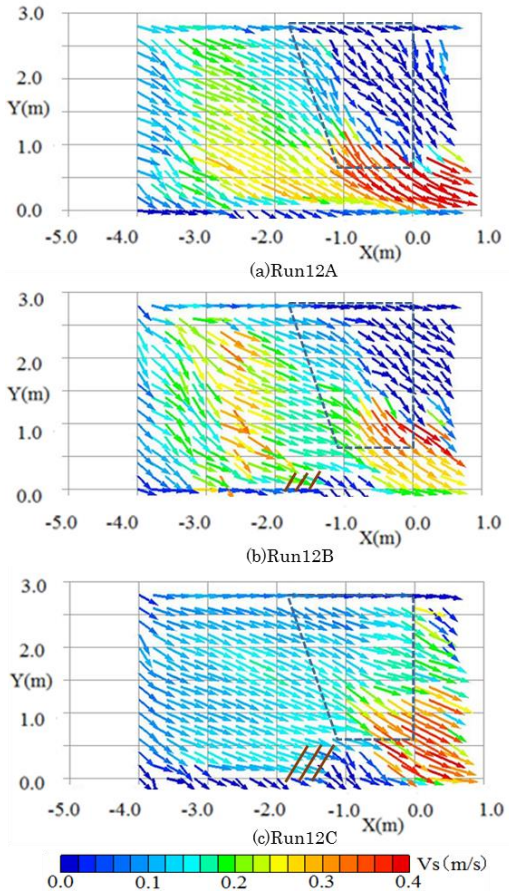

Figure 10. Surface velocity distributions around river-mouth bar

4. NUMERICAL SIMULATION

4.1 Simulation model and its governing equations

Since morphological changes of the river-mouth bar depend not only on the significant wave heights and water discharges but also the topography of its surrounding region, it is important to deal with a large area including the river-mouth bar. We investigate here the effects of the size of flood discharge on the river-mouth topography by means of the numerical simulation model.

The simulation model Nays2D (iRIC, 2013) was applied to the investigation in this study. The continuity equations of flow and sediment transport, and the momentum equations are

$$\frac{\partial h}{\partial t}+\frac{\partial (uh)}{\partial x}+\frac{\partial (vh)}{\partial y}=0 \quad [1]$$

$$\frac{\partial z}{\partial t}+\frac{1}{1-\lambda}\left(\frac{\partial q_{bx}}{\partial x}+\frac{\partial q_{by}}{\partial y}+q_{su}+w_f c_b\right)=0 \quad [2]$$

$$\frac{\partial (uh)}{\partial t}+\frac{\partial (hu^2)}{\partial x}+\frac{\partial (huv)}{\partial y}=-hg\frac{\partial H}{\partial x}-\frac{\tau_x}{\rho}+D_x \quad [3]$$

$$\frac{\partial (vh)}{\partial t}+\frac{\partial (huv)}{\partial x}+\frac{\partial (hv^2)}{\partial y}=-hg\frac{\partial H}{\partial y}-\frac{\tau_y}{\rho}+D_y \quad [4]$$

where x, y = plane Cartesian coordinates, u, v = velocity components in x and y directions, t = time, h = water depth, H = water elevation, g = gravity acceleration, ρ = fluid density, τ_x, τ_y = bed shear stress components in x and y directions, D_x, D_y = diffusion terms in x and y directions, z = bed elevation, λ = bed porosity, q_{bx}, q_{by} = bed-load sediment transport rates per unit width in in x and y directions, q_{su} = release rate of sediment from bed, w_f = settling velocity of sediment, c_b = reference concentration of suspended sediment.

The governing equations mentioned above and others are transformed into discrete forms in a generalized coordinate system. In the simulation model, the advection terms are discretized by the CIP method and the zero equation model is applied as a turbulence model. As for the sediment transport equation, the Ashida-Michiue equation for x direction and Hasegawa equation for y direction are employed in the model (Miwa et al., 2013).

4.2 Effects of size of flood discharge on erosion of river-mouth bar in the Yuragawa River

The contour line and the computational grid of the calculation area which is based on the bathymetric survey of October 2010 are shown in Figure 11. The longitudinal range of the area is -0.6 kp to 3.0 kp, and the area is divided into 25 grids for lateral direction and into 150 grids for longitudinal direction (the grid intervals of 20 m for -0.6 kp to 2.0 kp and them of 50 m for 2.0 kp to 3.0 kp). The mean grain diameter of the sediment was set to d_m = 0.3 mm and the Manning's

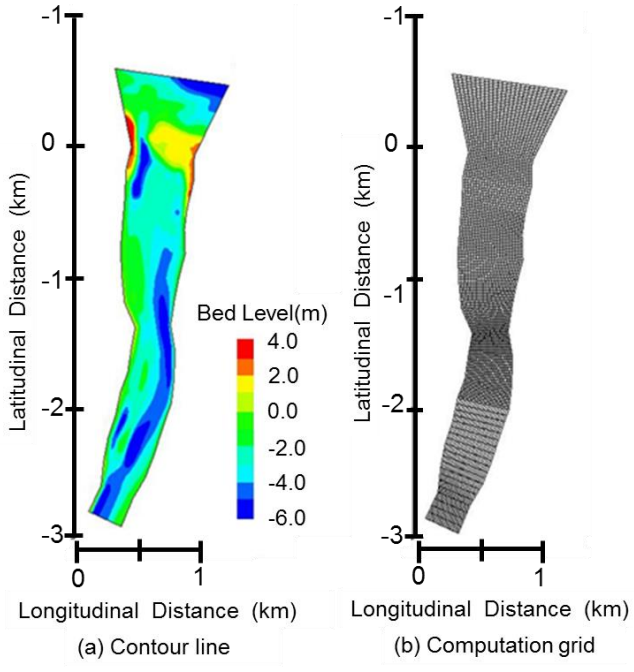

Figure 11. Contour line and computational grid of calculation area in the Yuragawa River

roughness coefficient is taken as n = 0.020. The water discharge conditions were set to five cases of Q = 1,500 to 3,500 m^3/s with intervals of 500 m^3/s. The duration time of the water discharge was taken as three hours. The sea level was given as h_d = 0.458 m of the high water level at the Maizuru Marine Observatory. The time increment (Δt) was taken as 0.01 second. In the computation, the water discharge and sea level were given at the upstream and downstream boundaries, respectively.

Figure 12 shows temporal variations in area, height and volume of the river-mouth bar. A_0, H_0 and V_0 in the vertical axis are the initial value of them, respectively. The bar area begins to decrease at Q = 2,000 m^3/s, and it considerably decreases at over Q = 3,000 m^3/s. The bar height also decreases at over Q = 2,000 m^3/s. The decrease rate reaches steady state at about an hour and it hardly change after that. Therefore, it can be considered that effect of the continuous high water discharge on the bar height is relatively small. Under the situation of decrease of the bar volume for each water discharge condition, the variation in the area shows similar tendency between Q = 2,000 and 2,500 m^3/s, and the variation in the height shows similar tendency between Q = 2,500 and 3,000 m^3/s. This result may mean that the changing mechanisms of the area and height of the bar on the erosion mechanisms of the mouth-bar are different each other by the amount of the water discharge.

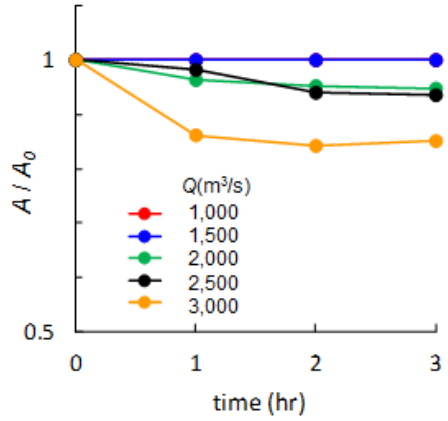

(a) Area

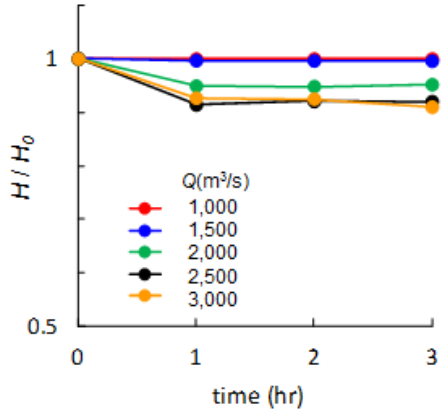

(b) Height

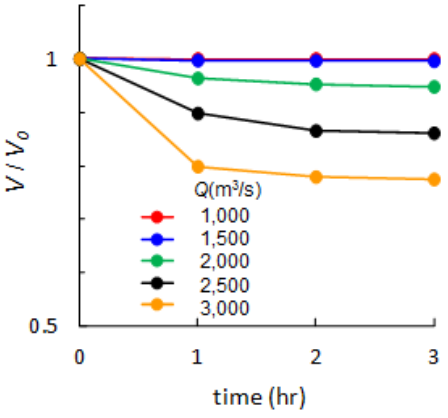

(c) Volume

Figure 12. Temporal variations in responses of river-mouth bars to flood discharge

4.3 River -mouth bar topography change due to flood discharge and its control by the spur dikes

Numerical simulations were conducted in order to further investigate the control method for the river-mouth bar topography. Nays2D, which is mentioned in Section 4.1, was used in the simulation. Rectangular coordinates are used in the simulation. The channel (5.68 m long, 2.84 m wide) was divided into 142 and 71 grids for the longitudinal and lateral directions, respectively. Then, the longitudinal grid size (Δx) and the lateral grid size (Δy) were the both 0.04 m. The Manning's roughness coefficient and the time increment were taken as n = 0.020 and Δt = 0.01 second, respectively. The value of h_d are set as 0.14, 0.13 and 0.13 m for Run 12A, Run12B and Run12C, respectively, in order to promote the bed variation. Other parameters and hydraulic conditions were the same as the experiments.

Figure 13 illustrates the reproduction calculation results of the flume experiments. The vectors mean the depth averaged flow velocities. The flow converges toward the river-mouth and the erosion of the river-mouth bar is relatively small in Run 12A. The flow around the spur dikes is redirected to the river-mouth bar. Therefore, the front part of the bar is eroded more in Run 12B and the width of the river-mouth channel becomes large. In Run 12C, the erosion of the river-mouth bar is more active, transported sediments are accumulated behind the bar like a sand spit. The scour of the river-mouth bar channel is restrained because the width of the channel becomes large. Although the flow gets over the river-mouth bar, the bar surface is hardly eroded in all Runs. These simulation results can reproduce most of the experimental results. However, the erosion of the bar surface in Run12C cannot be reproduced in the simulation. This problem may be caused by the boundary condition at the downstream end of the channel.

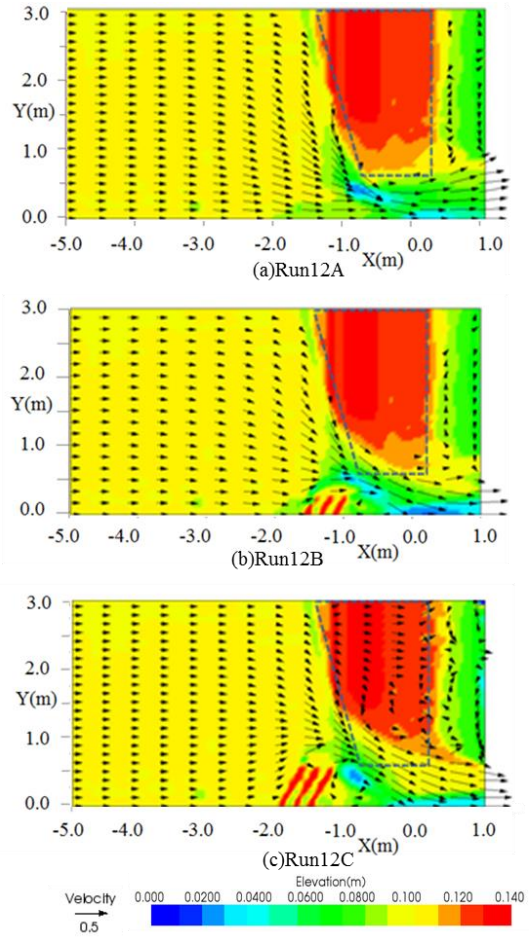

Figure 13. Reproduction calculation results of flume experiments

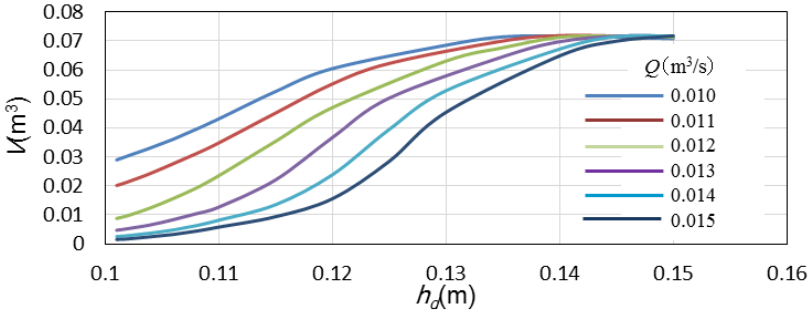

Figure 14. Relationship between downstream-end water level and bar volume (spur dike length: 30 cm)

Using a spur dike length of 30 cm, which yielded good reproducibility in the experimental results, we performed calculations by varying the parameters of downstream-end water level and water discharge. As shown in the relationship between the downstream-end water level and the volume of the river-mouth bar after water passage in Figure 14, the bar volume decreased with decreasing downstream-end water level and increasing water discharge. In cases where the downstream-end water level was high and the bar overflow was sufficiently large, the bar volume after water passage exhibited little or no dependence on water discharge..

5. CONCLUSIONS

The results obtained in this study are summarized as follows:

(1) Although the bar area and volume of the river-mouth bar showed short-term fluctuations due to flooding, they also showed a tendency to increase on a long-term basis. The flush condition of the river-mouth bar sediments due to flooding does not depend on the width of river-mouth channel and the bar area but on flood discharge. The formation of the river-mouth bar may be mainly activated by an increase of longshore sediment transport rate in winter season; the bar area has a strong correlation with wave height.

(2) The movable-bed experiments showed that, in the region upstream of the bar, a meandering flow from near the right bank toward the bar channel predominates. Associated with the formation of the meandering channel, the flow converges in the channel region and a deeply scoured topography develops in the region upstream of the bar tip. The experiments also showed that both the water-surface gradient over the bar and the channel width increase as the downstream-end water level decreases and the water discharge increases.

(3) In the experiment without spur dikes, the scour depth of the river-mouth channel became large because of the flow converging into the channel. On the other hand, in the experiments with the spur dikes, the erosion of the river-mouth bar became active and the scour depth of the river-mouth channel became small because of the spur dikes redirecting the flow toward the river-mouth bar. Sediments deposited at the lower part of the spur dikes because the flow intensity was weak there.

(4) The simulation results showed that the bar area and height of the river-mouth bar considerably decrease in the early stage of the flood period, and that the decrease rate after that is relatively small. Over 3,000 m^3/s of flood discharge accelerates the erosion of the bar, and it also decreases its area remarkably. The mechanisms of the flow which takes the long way around the spur dikes, and the river bed variation process were clarified by the reproduction calculations of the experiments.

ACKNOWLEDGMENTS

This study is financially supported by the Fukuchiyama Work Office of the Ministry of Land, Infrastructure, Transport and Tourism, Japan. Hideka Murakami (Kyoto University) and Kotone Yamasaki (NTT Infrastructure Network Corp.) provided valuable help in conducting the research. The authors express their gratitude to them.

REFERENCES

Fujita, I., Hara, M., Morimoto, T. and Onishi, T (1998). Application of PIV techniques to measurement of river surface flows. *Advances in River Engineering*, 4, 41-46, (in Japanese).

Hosoyamada T., Sato K., Noda T., Sakai M., and Sakamukai H. (2006). A numerical study for flashing of sandbars by flood in the Agano River mouth. *Advances in River Engineering,* 16, 73-78, (in Japanese).

International River Interface Corporative (2013). Guide Book on iRIC Seminar in KANSAI, (in Japanese).

Iwagaki Y. (1956). Hydro dynamical study on critical tractive force. *Journal of J.S.C.E.* 41, 1-21 I, (in Japanese).

Kanda, K., Miwa, H. and Kato, Y. (2012), Study on dynamic status of river-mouth topography and its control methods in Yuragawa River,*Research report on the Grant-in-Aid for Technical Research Development of River and Erosion-control Technology*, MLIT, (in Japanese).

Kuwahara N., Tanaka H., Sato K., and Shuto N. (1996). Field application of a numerical model for river mouth topography change. *Annual Journal of Hydraulic Engineering*, 40, 953-958, (in Japanese).

Miwa H., Kanda K., Yamasaki K., Ochi T., and Murakami H. (2014). Observing dynamic state of river-mouth bar and its control in the Yuragawa River. *Proceedings of I.C.H.E,* 16, CD-ROM.

Sato T., Suprijo T., and Mano A. (2004). Equilibrium condition at the narrowest section of the major rivers with sand spits. *Proceedings of 26th Coastal Engineering Conference*, 51, 526-530, (in Japanese).

Tateyama M., Yamasaki T., Tanabe M., Uchida T., and Fukuoka S. (2013). Study on the new analysys method flushing of the river mouth sandbars by the flooding. *Advances in River Engineering,* 16, 247-252, (in Japanese).